Anuário do Instituto de Geociências - UFRJ
www.anuario.igeo.ufrj.br

Mapping of a Paleochannel Through a Geoelectric Survey

Mapeamento de um Paleocanal por Levantamento Geoelétrico

Paula Rayane Lopes de Andrade & José Agnelo Soares

Universidade Federal de Campina Grande;
Rua Aprígio Veloso, 882 – Bairro Universitário, 58429-900, Campina Grande, Paraíba, Brasil
E-mails: ufcgpaulaandrade@gmail.com; agnelosoares@gmail.com
Recebido em:19/11/2018 Aprovado em:29/03/2019
DOI: http://dx.doi.org/10.11137/2019_2_184_196

Abstract

This paper presents the results of a survey of electric resistivity along a stretch of the Sucuru River, in the vicinity of the Sumé city, in the Northeast region of Brazil. The goal is to map the occurrence of sediments saturated with water whose main paleochannel is a suitable feature for drilling water-producer wells. Two manual Auger coring surveys were made with pick up of sediment samples for petrophysical tests and record of six 2D lines of electric resistivity, applying multiple vertical electric soundings, which were interpolated to generate a 3D electrical resistivity model of that part of the river. The results show that the fine sediments tend to have low values of electrical resistivity (lower than 50 ohm.m), except on non-saturated region, while intervals with lithotypes of high grain sizes tend to present resistivity values between 50 and 200 ohm.m, except in regions of high porosity and high water saturation. In general, it is seen that there is an area with resistivity higher than 200 ohm.m at the top, which corresponds to the non-saturated sediments zone, and another at the base, which corresponds to the crystalline basement. The model allows someone to view, in addition to the main paleochannel, secondary channels, which hardly would be completely identified through a regular core drilling program.
Keywords: Hydrogeophysics; paleoclimate; buried paleochannel

Resumo

Este artigo apresenta os resultados de um levantamento de resistividade elétrica ao longo de um trecho do Rio Sucuru, nas proximidades da cidade de Sumé, na região do cariri paraibano. O objetivo é mapear a ocorrência de sedimentos saturados de água cujo principal paleocanal é uma estrutura adequada para a perfuração de poços produtores de água. Duas sondagens a trado manual foram realizadas com a extração de amostras de sedimentos para ensaios petrofísicos e foram registradas seis linhas 2D de resistividade elétrica, usando múltiplas sondagens elétricas verticais, as quais foram interpoladas para gerar um modelo 3D de resistividade elétrica daquele trecho do rio. Os resultados mostram que os sedimentos finos tendem a ter baixos valores de resistividade elétrica (menores que 50 ohm.m), exceto na região não-saturada, enquanto intervalos com litotipos de tamanhos de grãos grandes tendem a apresentar valores de resistividade entre 50 e 200 ohm.m, exceto nas regiões de alta porosidade e alta saturação de água. Em geral, vê-se que há uma área com resistividade acima de 200 ohm.m no topo, que corresponde à zona de sedimentos não-saturados, e outra na base, que corresponde ao embasamento cristalino. O modelo permite, além de identificar o paleocanal principal, visualizar também paleocanais secundários, os quais dificilmente seriam claramente identificados por um programa regular de sondagem.
Palavras-chave: Hidrogeofísica; paleoclima; paleocanal soterrado

1 Introduction

The study of alluvial plains is important in the hydrogeological search, as well as the paleochannel recognition and the sedimentary evolution of these plains. Over time, processes such as climate change and weathering cause reallocation and resizing of river channels. Old channels are filled with sediments and they act as preferential paths to groundwater flow.

The recognition of paleochannels is an important element in the construction of the evolutionary process of fluvial systems. Paleochannels provide information about paleoclimate, possible mineral occurrences associated with fluvial dynamics and hydrogeological favorability. Due to the constructive process itself, paleochannels do not present clear evidence in the local relief, so they are not easily recognized on the surface of the terrain. The methods used in the recognition of paleochannels are varied, such as the use of multispectral images (Gilvear & Bryant, 2003), digital elevation models (Almeida Filho & Miranda, 2007) and synthetic aperture radar images (Rossetti, 2010). Several authors have used geophysical techniques for the recognition of paleochannels. Luciano & Harris (2013) applied ground penetration radar (GPR) to the mapping of paleochannels in an area of South Carolina, USA. Genau et al. (1994) applied the seismic method of reflection, of high resolution and low depth of investigation, to map quaternary paleochannels in Maryland, USA. Fradelizio et al. (2008) used 3D seismic imaging to identify the margins and the bottom of a paleochannel inserted between 10 and 15 meters deep in a layer of clay. Islam et al. (2016) used vertical electrical survey and electrical conductivity (electromagnetic survey) to map a paleochannel in the Cholistan desert of Pakistan and evaluate the quality of groundwater present in it.

Classic hydrogeological information has been increasingly complemented with subsurface geophysical information that allows obtaining more accurate images of aquifer systems (Schwinn & Tezkan, 1997; Unsworth et al., 2000; Krivochieva & Chouteau, 2003; Meju et al., 2003; Kafri & Goldman, 2005; Pedersen et al., 2005; Mota & Monteiro dos Santos, 2006). Falgàs et al. (2011) characterize the complex lithological structure and the seawater intrusion state by combining hydrological information, audiomagnetotelluric (AMT) data and seismic reflection and refraction models. Thus, they have determined the thickness and continuity of the aquifer units, as well as the morphology and depth to the basement. The models revealed that the seawater intrusion main path is found in the western deltaic area that coincides with an existing buried paleochannel.

This work investigates an alluvial deposit saturated in water located along the Sucuru riverbed, which consists of an intermittent river located in the semi-arid region of northeastern Brazil. The units that make up this deposit were mapped through the application of the electro resistivity geophysical method. Figure 1 shows the location map of the study area, indicated by the yellow rectangle, which measures 125 m long by 100 m wide. The studied area is within an irrigated perimeter which uses wells to satisfy the water demand.

The irrigated perimeter of Sumé is located in an area where the semi-arid climate predominates, characterized by annual precipitation below 500 mm, high temperatures, strong evaporation and alternation of two distinct seasons: the rainy, also called winter, and the drought, or summer. With respect to rainfall, it occurs between January and July, with higher intensity in the months of March and April. The average annual temperature is 24° C, with maximum between November/December and minimum in July/August. The average annual relative humidity is 57%. The annual evaporation is 2800 mm in tank class A (DNOCS, 2018; Cadier, 1994; Albuquerque, 2002).

The native vegetation of the site is a dense hyperxerophilic caatinga with stretches of deciduous forest and thorny shrub, herbaceous plants and cactus, as well as few sparse trees and shrubs, not been a continuous vegetation cover (Barros, 2010; Albuquerque, 2002).

Soils are part of a valley embedded geologically in the Brazilian crystalline complex. The predominant types of soil are ortic chromic luvisol and eutrophic fluvic neosol, formed from granite and

gneiss with quartz veins. The soils of the irrigated perimeter area are largely of eutrophic alluvial origin, deposited by the Sucuru River and its tributaries, without uniformity in its distribution (EMBRAPA, 2006). These soils are considered suitable for the practice of irrigation because of the high natural fertility. Eutrophic alluvial soils are found in floodplain areas on the banks of watercourses, being highly evident on the banks of the Sucuru River. The perimeter area presents a flat topography with slight gradients (Júnior et al., 2009; Silva, 2006; DNOCS, 2018).

Alluvial aquifer systems represent a valuable alternative in the Brazilian semi-arid region, whether for domestic use, animal watering or irrigation, since in the dry season the surface water supply becomes restricted. According to Montenegro et al. (2003), water stored in alluvial aquifers has been the main source of supply for the development of small-scale agriculture, as well as family farming, which represents a great potential contribution to regional socioeconomic equilibrium.

Downstream of the Sumé superficial water reservoir is located, along the course of the Sucuru River, the alluvial aquifer. The widths of the alluvial deposits occurring in the perimeter range between 100 m and 350 m and the thicknesses of the alluvial package vary between a minimum of 0.45 m and a maximum of 9.30 m with an average thickness of 4.25 m (Vieira, 2002). That author carried out a mapping of 49 water points in the irrigated perimeter, most of them rudimentary excavations without coverings, up to 3 meters deep, which indicated the underlying presence of an alluvial aquifer.

2 Regional Geology

The study area is located along the Sucuru riverbed, about 1 km downstream from the city of Sumé, as shown in Figure 1. The region is located in the Borborema Province and the predominant lithotypes in the area are quaternary sedimentary coverages which overlap the basement composed of granitic-granodioritic and tonalitic migmatized rocks with predominance of orthogneisses (CPRM, 2000).

According to CPRM (2000), alluvial deposits occurring in the area are small, with some exceptions for those located in certain sites along the Paraíba River. They consist mainly of sands of varying granulometry and clays in places where the rivers present

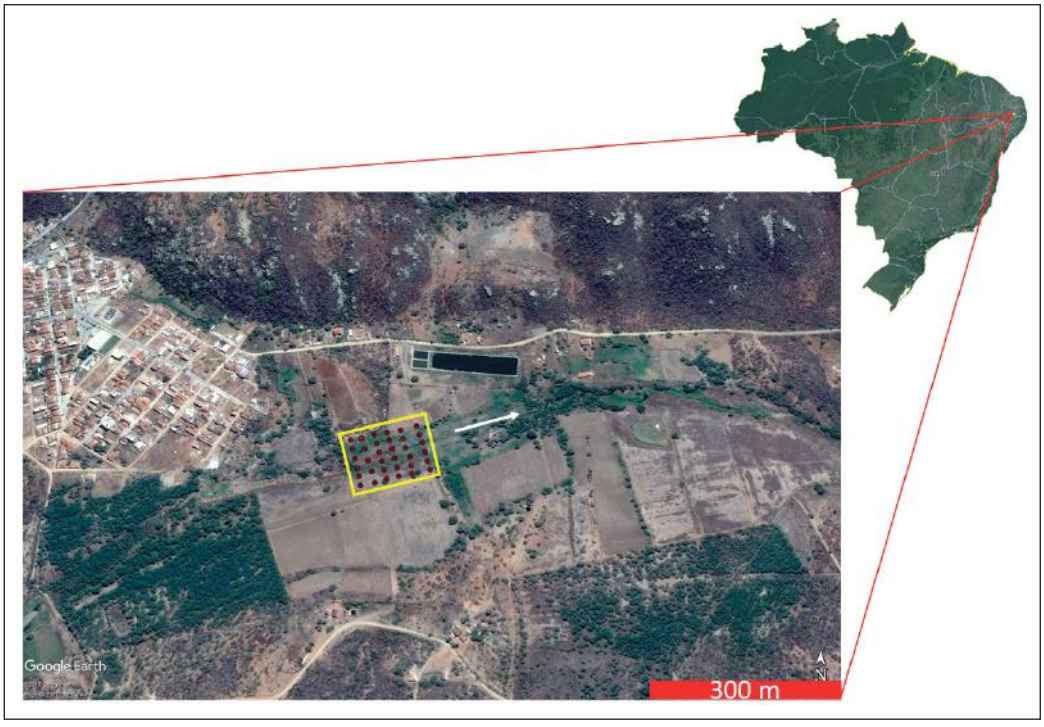

Figure 1 Location of the study area (yellow square), near Sumé city. The white arrow shows the river water flow direction. Red circles show the center position of vertical eletroresistivity soundings.

a greater flood plain, forming clayey soils with a few meters of thickness.

The aquifer in the study area consists of a free, non-draining granular aquifer composed of sand grains, silt and clay. Alluvial aquifers are geological formations with deposits of recent origin (or quaternary) originated from the processes of development of rivers and streams occurring on the surface of a hydrographic basin, forming streams and flood plains.

In the semi-arid region, most of the areas present a weak hydrogeological potential, with a low water accumulation and circulation capacity, due to the predominance of the crystalline basement and the low rainfall rates in the region, together with the high evapotranspiration rates and unfavorable geology for groundwater exploitation. Due to the geological formation process, the alluvial aquifers of the Northeastern semi-arid region are shallow, narrow and elongated, functioning as groundwater conduits.

For the semi-arid region, alluvial aquifers are often the only source of supply available in many small communities and are presented as a real alternative for minimizing the effects of drought and are used for multiple uses, ranging from supplying small communities to extensive use in family agriculture (Salgado, 2016).

3 Methodology

For the evaluation of the spatial distribution of the flow units that make up the analyzed aquifer, static water level meters were installed in drilling holes with recovery of sediment samples for mineralogical and granulometric description and petrophysical tests. Geophysical data were acquired through the method of eletroresistivity. Afterwards 2D data inversion an interpolation of geophysical data were done for the generation of the 3D model of the analyzed aquifer section.

3.1 Recovery of Core Drill Samples

In the study area, two boreholes were drilled manually with recovery of sediment samples for mineralogical and granulometric description, as well as petrophysical tests. The measured properties were porosity, grain density and total density. The drill holes were used to measure the static water level. The maximum depth of the samples of coring 1 was approximately 3.80 m, while the coring 2 reached 6.0 m depth.

3.2 Petrophysical Tests

The sediment samples collected during the drilling process are unconsolidated. To perform petrophysical tests, it is necessary to pre-encapsulate these samples in order to leave them in the required shape and size. For this purpose, cylindrical capsules composed of aluminum sheets with stainless steel screens at both ends were produced. It was used a 200 mesh screen. The capsules (Figure 2), with dimensions of 38 mm in diameter by about 5 cm in length, were filled with the sediments and compacted under 300 psi in a triaxial confinement cell. They were then oven dried at 80° C for 24 hours.

Figure 2 Example of prepared sediment samples before their compaction.

After drying the samples were weighted and their dimensions (length and diameter) were measured in a digital pachymeter. The porosity and grain density test is performed on the Ultraporoperm 500 equipment (Figure 3), connected to a matrix cup. This test consists in introducing nitrogen gas into a hermetically sealed matrix cup, whose volume is known, and which contains the sediments sample in its interior. When necessary, steel discs are added to save nitrogen when the sample is much shorter than the cup.

The gas, initially held within the permoporosimeter at known volume and pressure, is released to expand through the voids within the matrix cup,

Figura 3
Corelab Ultraporoperm 500 device (Apolinário, 2016).

which includes the pores of the sediments sample. This expansion results in a drop in gas pressure, whose new value is measured. Since the volume of the matrix cup is known, the new volume occupied by the gas corresponds to the difference between the volume of the cup and the grain volume, which is directly determined.

In order to obtain the porosity of the sediments, it is assumed that the sample under analysis is totally dry, then porosity can be determined as the ratio between the pore volume and the sample total volume. The sample is dried, then its grain density can be calculated as the ratio of the sample mass to its grain volume. The total density of the sample is given by the ratio of the mass of the sample to its total volume.

3.3 Geophysical Survey

In the geophysical investigation the eletroresistivity method was applied with the acquisition of multiple VES (vertical eletroresistivity sounding) along 2D data lines, using the Schlumberger array of electrodes. The location of the study area is indicated by the yellow rectangle in Figure 1, which measures 125 m in the Y axis direction by 100 m in the direction of the X axis. The equipment used was a Bodenseewerk Geosystem model GGA 30, as shown in Figure 4. Center position of each VES is indicated in Figure 1 as a red circle. The six 2D lines were acquired in the direction perpendicular to the Sucuru river.

Figure 4 Device used for the eletroresistivity survey.

In the investigated area, as indicated in Figure 1, six resistivity lines were spaced by 25 m, where for each line six VES with spacing of 20 m were made. The spacing used between the current electrodes was 10 m and between the potential electrodes was 2 m. The total size of each line was 200 m, and for each VES, a maximum distance of 100 m between the current electrodes was adopted.

The data acquisition was performed in the form of lines arranged in the direction X perpendic-

Anuário do Instituto de Geociências - UFRJ
ISSN 0101-9759 e-ISSN 1982-3908 - Vol. 42 - 2 / 2019 p. 184-196

ular to the axis of the river channel (Y direction). Each line starts at position X = -50 m (see Figure 1) and ends at position X = 150 m. However, geoelectric sections were generated only in the region between the centers of the first and sixth VES of each line, thus each geoelectric section starts at X = 0 m and ends at X = 100 m. The lines were recorded for successively increasing Y positions, from Y = 0 m to Y = 125 m. The terrain topography is relatively flat, presenting only sub-metric depressions in areas located at the center of the river channel. Such topographical variations were neglected in this study.

The data inversion was performed through Res2Dinv software for each individual data line, being each line composed by six VES. The least squares inversion method was applied to each set of six VES resulting in geoelectric sections with approximately 20 meters of maximum depth of investigation. It was adopted five as the maximum number of interactions for data inversion and there was not bad points removal.

A three-dimensional model for the studied area was generated through the application of a space discretization process by a mesh of cells. For the interpolation of the two-dimensional sections, the inverse of the squared distance, with anisotropic data search, was applied. The length axis for the search ellipse was 25 m, 62.5 m and 5 m, for x, y and z directions, respectively. The minimum and maximum number of data to be considered within the search ellipsoid were respectively 3 and 50.

4 Results and Discussions

Figure 5 shows the lithostratigraphic profiles for the two core drills. The colors represent the grain size classes. In the upper half of core 1 predominantly occurs medium and medium to fine sands, whereas in the lower half predominate very coarse sand, pebbles and granules. In core 2 down to the depth of 4 meters, sediments with grain size up to fine sand occur, while below this depth coarse sands to pebbles predominate. The maximum depth of each core drill was limited by the maximum penetration reached by the manual drilling device.

Figures 6 and 7 present the profiles of the petrophysical properties measured for samples from core drills 1 and 2, respectively. In these profiles it is observed that in the shallower facies (silt and fine to average sand) higher values of grain density occur, indicating a composition that includes more dense minerals. The clays present low to medium grain density and low porosity. The pebbles present low grain density and medium to high porosity.

Figure 8 shows the relationship between the total density and the porosity of the samples from drillings 1 and 2. In this figure three trend lines are observed, according to grain size and mineral composition. Line A corresponds to the samples with high particle size, the line B to the samples of fine particle size and the line C to the samples also of fine particle size but containing minerals more dense than the quartz.

Figure 9 shows that the samples 01_01, 02_01 and 02_03A have grain density above 2.7 g / cm³, while the others have grain density around 2.65 g / cm³. The latter should be composed mainly by quartz, while the former contain minerals substantially more dense than quartz.

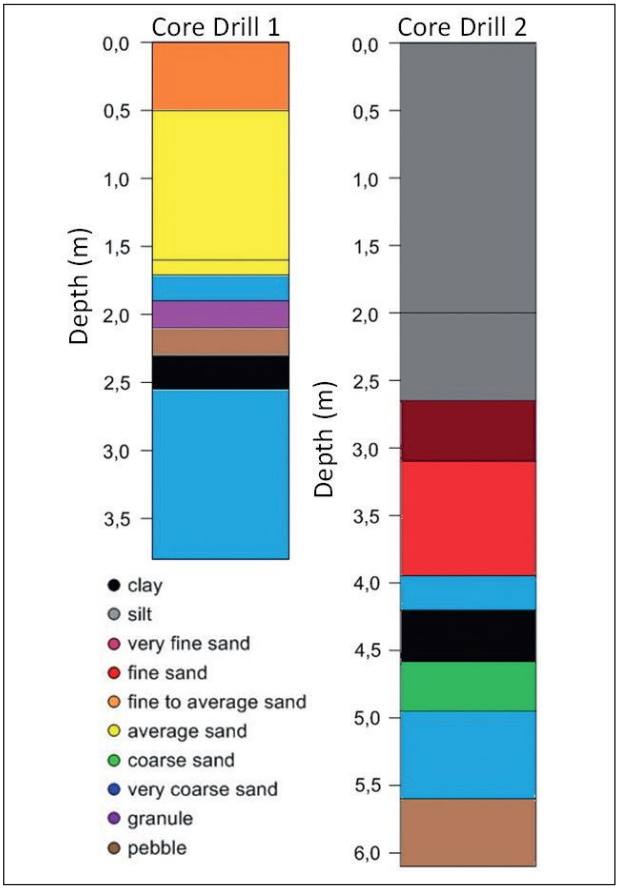

Figure 5 Lithostratigraphic profiles of the two core drills made at the study area.

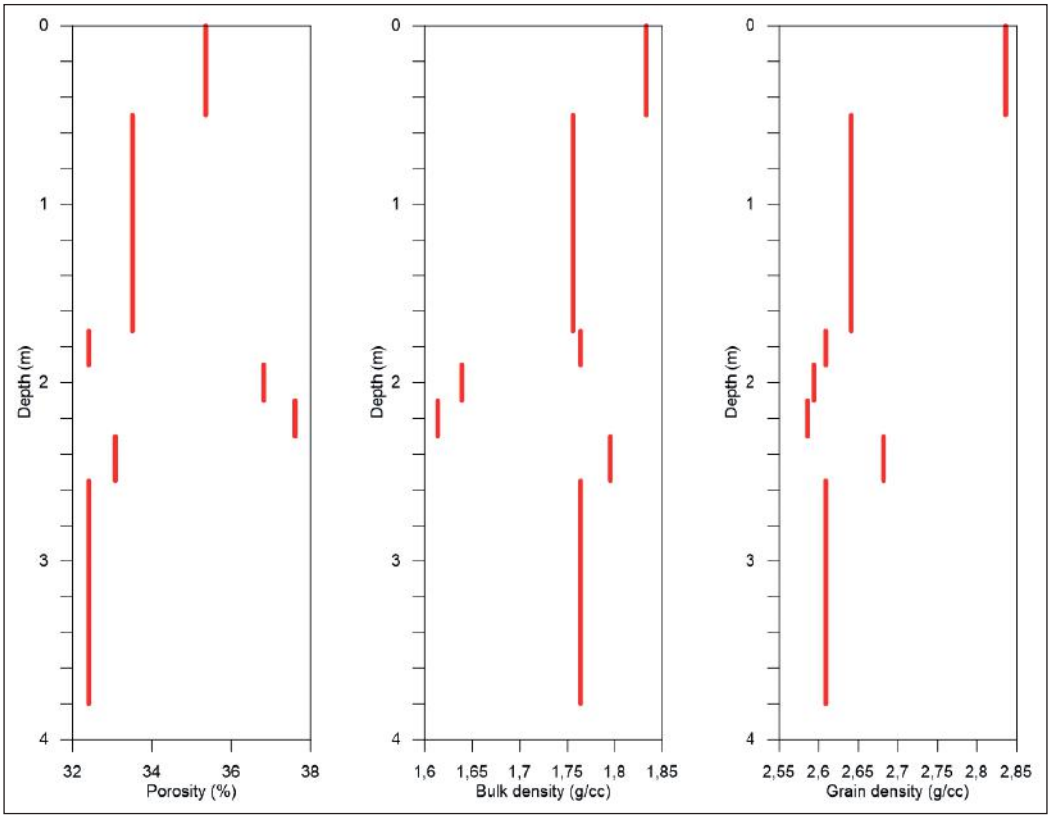

Figure 6 Petrophysical profiles for core drill 1.

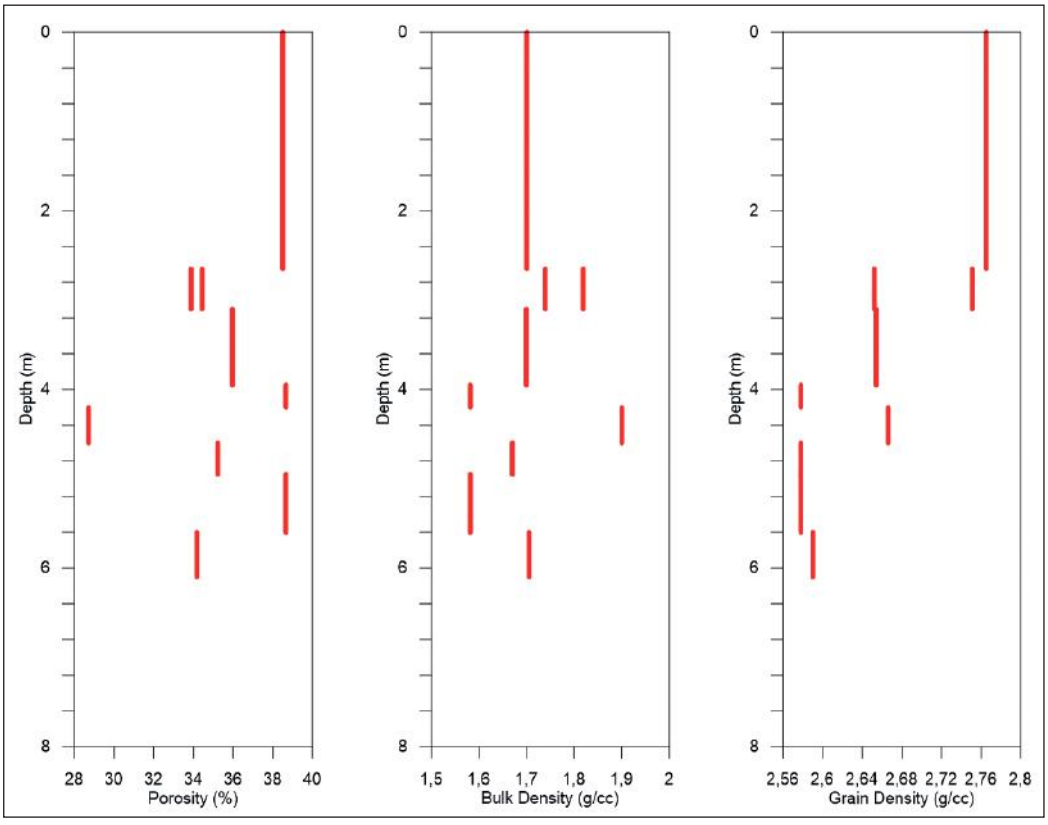

Figure 7 Petrophysical profiles for core drill 2.

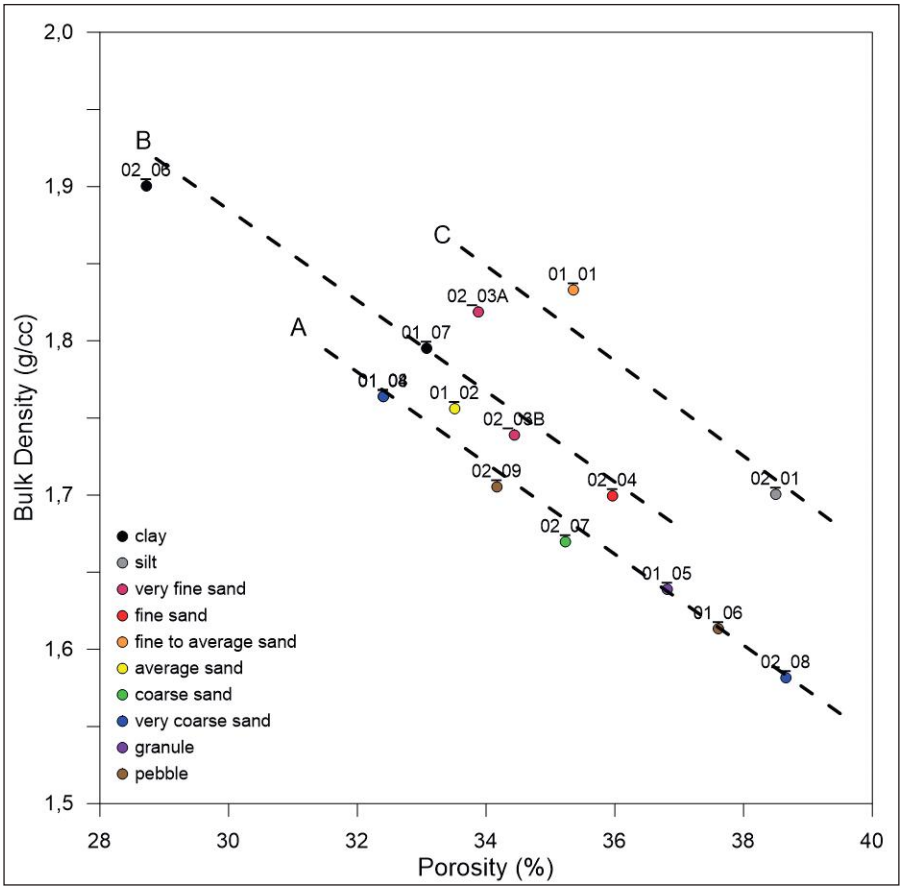

Figure 8 Relationship between total density and porosity. Line A corresponds to the samples with high particle size, line B to the samples with fine particle size and line C to the samples containing minerals more dense than quartz.

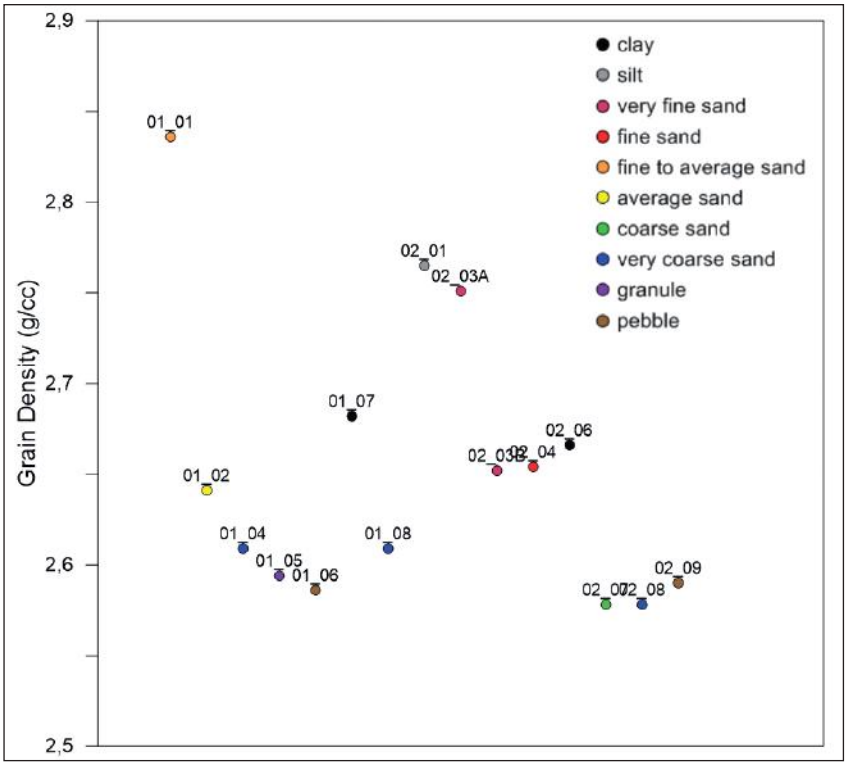

Figure 9 Grain density measured in samples from core drills 1 and 2.

Six 2D resistivity geoelectric sections were obtained by inverting the data from each recorded line. The RMS errors obtained in the inversion of each line are presented in Table 1. The errors found, all below 30%, were considered acceptable, and a considerable reduction in the error for lines 03 to 06 is observed.

Line	RMS (%)
01	29.1
02	26.7
03	15.7
04	18.2
05	16.8
06	15.1

Table 1 RMS error obtained in data inversion for each line.

Figure 10 shows the set of geoelectric sections positioned spatially in relation to the adopted system of axes. In this figure all the sections are in the same color scale. In general, there is a predominance of resistive regions (orange color) in the upper portion of the sections (small z-axis values), as well as in the lower left region (high x-axis values). On the other hand, the conductive region (white color) is predominantly in the right (small x axis) and in the central regions of the geoelectric sections.

Figure 11 presents the interpolated 3D model for the entire studied area. In this image the presented resistivities are limited to 200 ohm.m, because above this value it is not expected that sediments saturated by water occur (Braga, 2016).

Figures 12, 13 and 14 show, respectively, the granulometry, porosity and total density of the two core drills in relation to the 3D model of electrical resistivity. The colors and the diameters of the core profiles indicate the values of these petrophysical properties. In Figure 12 it can be observed that in the shallower interval of the core drill 2 (silt) low values of electrical resistivity (blue region) occur and that the intervals with lithotypes of greater granulometry present high values of resistivity.

Figure 13 shows that in the higher porosity regions low values of electrical resistivity predominate, while regions with lower porosity are associated with more resistive zones. This effect is associated with water saturation, because more porous regions have a higher water storage capacity, therefore they are more conductive. Regions with lower total density lithotypes are associated with those with higher porosity, therefore, with lower electrical resistivity. The higher grain density in the shallower lithotypes does not substantially affect these relationships among total density, porosity and resistivity. This

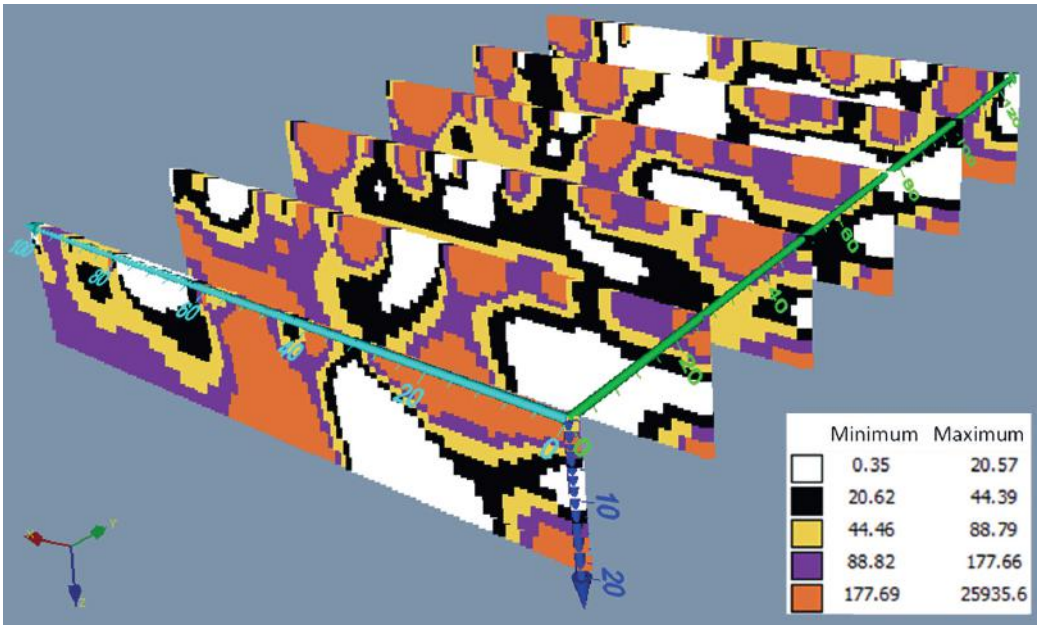

Figure 10 Inverted geoelectric sections spatially positioned in relation to the axis system. The number lines are increasing (1 to 6) with the increase of their Y axis position.

Anuário do Instituto de Geociências - UFRJ
ISSN 0101-9759 e-ISSN 1982-3908 - Vol. 42 - 2 / 2019 p. 184-196

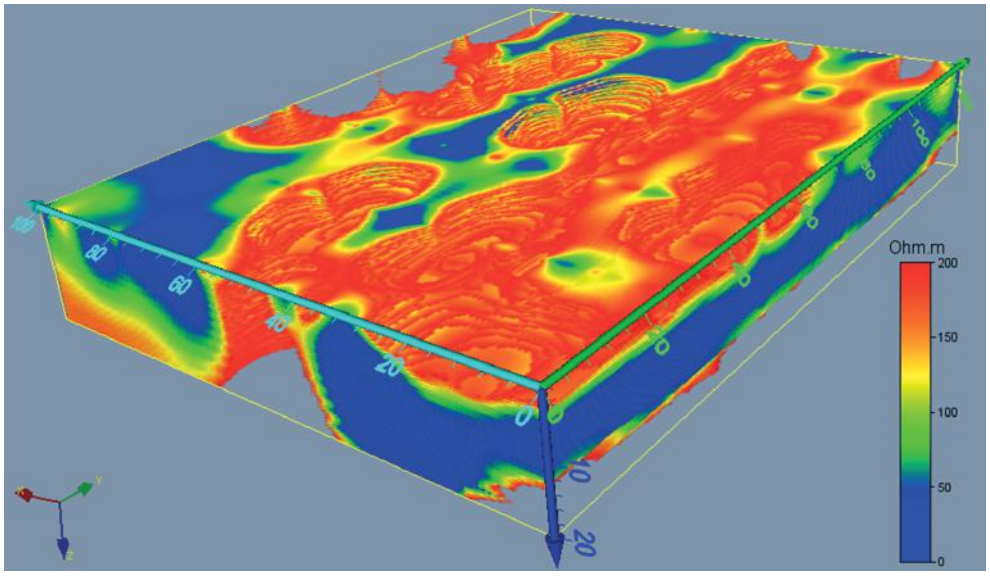

Figure 11 3D model of electrical resistivity of the study area.

is because the electrical resistivity of the mineral grains is always high, regardless of their density.

As discussed above, regions of low electrical resistivity are associated with higher water saturation or, alternatively, regions with predominance of clay minerals.

Figures 15 and 16 show cuts of the model in the XY plane at depths of 10 m and 17 m, respectively. In them it is observed that the saturated sediments of low resistivity (blue color) are concentrated along a linear region around the position X = 24 m. This conductive region indicates the position of the main paleochannel buried in this part of the Sucuru River. Unlike the maximum depth indicated by Vieira (2002), the maximum depth of the sediments along the paleochannel identified in this work is around 20 meters.

Figure 17 shows the surfaces that separate the zones with electrical resistivity higher and lower than 200 ohm.m, since this value is considered as the maximum resistivity expected for sediments saturated with water. In general, it is seen that there is a resistive zone at the top, which corresponds to the sediments of the unsaturated zone, and another at the base, which corresponds to the top of the crystalline basement.

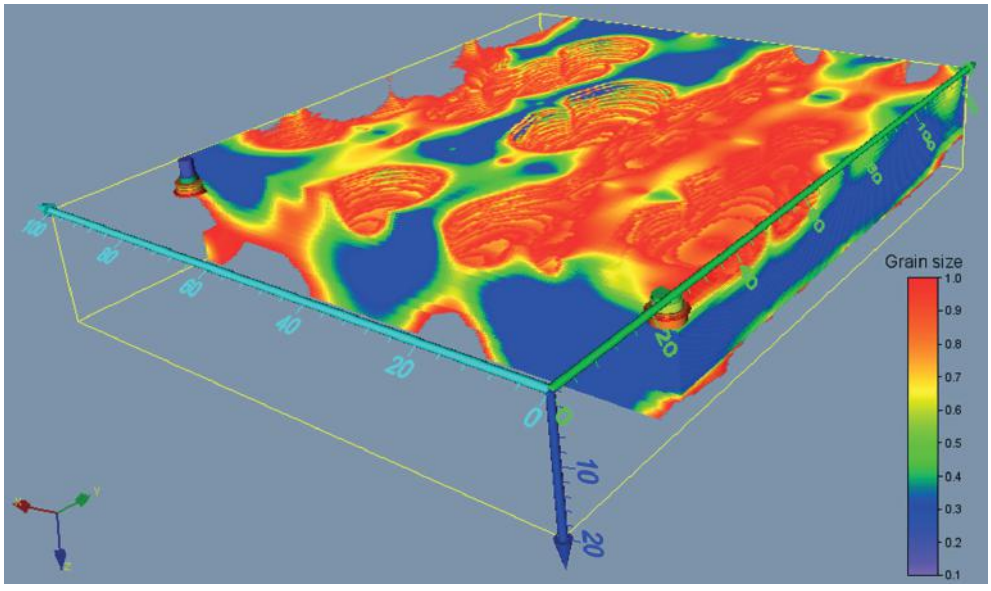

Figure 12 Granulometry profiles of the two core drills in relation to the 3D resistivity model.

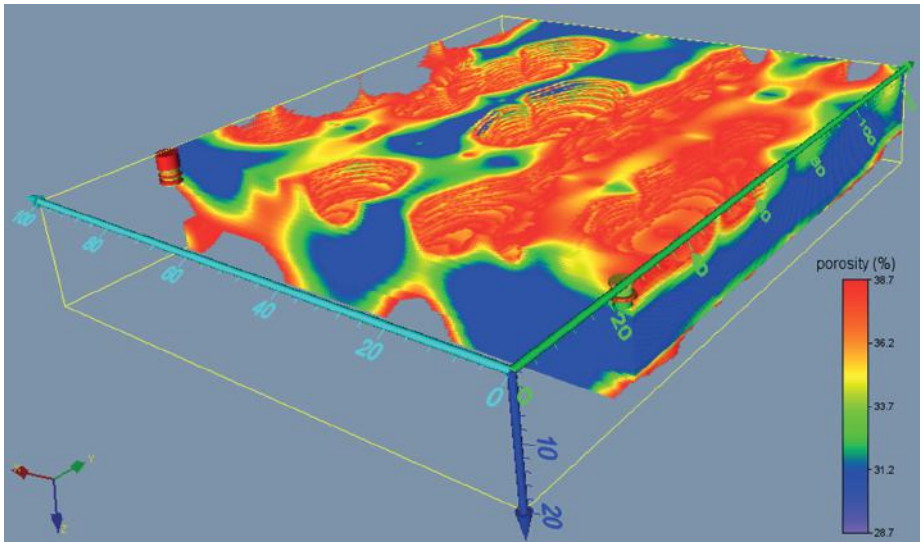

Figure 13 Porosity profiles of the two core drills in relation to the 3D resistivity model.

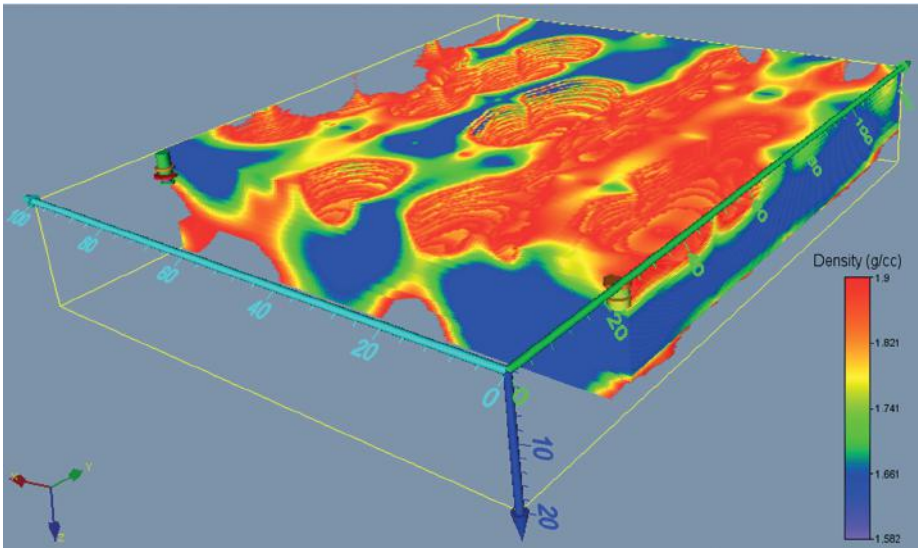

Figure 14 Total density profiles of the two core drills in relation to the 3D resistivity model.

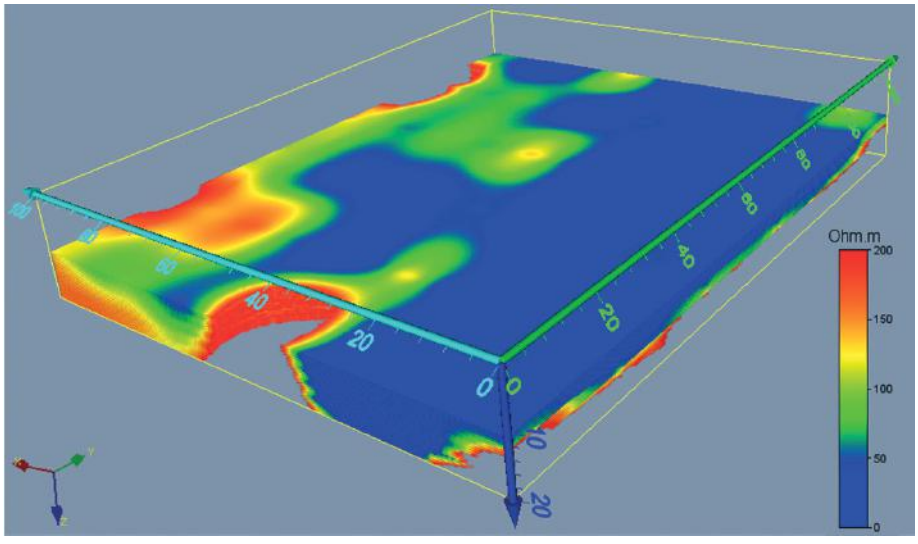

Figure 15 Cut of the 3D model of electrical resistivity in the depth of 10 m.

Anuário do Instituto de Geociências - UFRJ
ISSN 0101-9759 e-ISSN 1982-3908 - Vol. 42 - 2 / 2019 p. 184-196

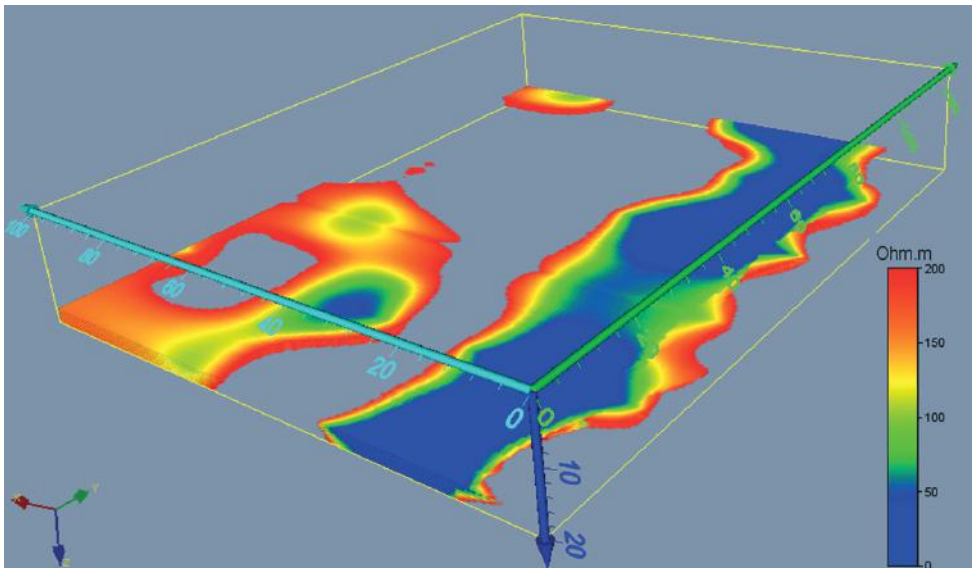

Figure 16 Cut of the 3D model of electrical resistivity at depth of 17 m.

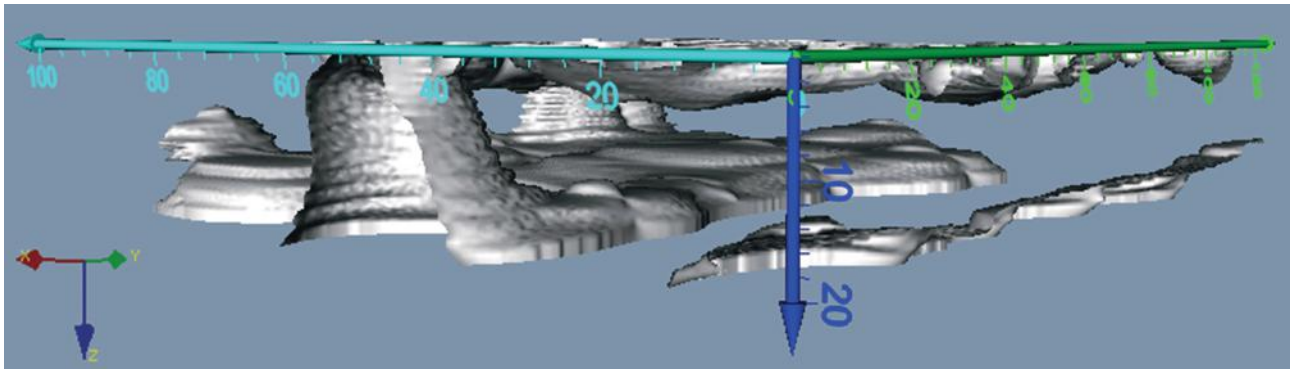

Figure 17 Electrical resistivity surfaces greater than 200 ohm.m. In this figure the paleochannel is clearly indicated in the lower right, the top of the basement to the left and right of the paleochannel and the surface resistive zone, which corresponds to the zone above the water level.

5 Conclusions

In this work the electrical properties of sediments were related to their petrophysical properties in order to support the interpretation of the geophysical model. The petrophysical properties show that in the shallower part of the sediments, minerals are denser than the quartz, which predominates in most of the sediments of the area. At the top of the core drills there is a predominance of fine sediments, while in the lower part predominate sediments of larger grain size. The fine sediments tend to present low values of electrical resistivity (lower than 50 ohm.m), except in the unsaturated region, whereas the intervals with lithotypes of larger granulometry tend to present resistivity values between 50 and 200 ohm.m, except in regions of high porosity and high water saturation. Regions with lower total density lithotypes are associated with those with higher porosity, therefore, with lower electrical resistivity. The higher grain density in the shallower lithotypes does not substantially affect these relationships among total density, porosity and resistivity. May be identified one area at the top with resistivity values higher than 200 ohm.m, which corresponds to the non-saturated sediments zone, and another at the base, which corresponds to the crystalline basement.

The eletroresistivity method proved to be adequate for the identification and quantification of the main paleochannel buried in the riverbed. This feature is visually identified in the 3D model as a

linear structure of low electrical resistivity due to its high porosity and saturation in water. The maximum depth of saturated sediments, unlike previously reported in the literature, reaches up to 20 m in the center of the main paleochannel. The generated 3D model allows to visualize, in addition to the main paleochannel, secondary channels, especially on the left side of the model, which would hardly be completely identified by means of a regular core drill program. The identification of paleochannels provides information about the paleoclimate, possible mineral occurrences associated with fluvial dynamics and optimizes the location of wells to be drilled with the objective of producing groundwater.

6 References

Albuquerque, A.W.; Lombardi Neto, F.; Srinivasan, V.S. & Santos, J.R. 2002. Manejo da cobertura do solo e de práticas conservacionistas nas perdas de solo e água em Sumé, PB. Revista Brasileira de Engenharia Agrícola e Ambiental, 6: 136-141.

Almeida Filho, R. & Miranda, F.P. 2007. Mega capture of the Rio Negro and formation of the Anavilhanas Archipelago, Central Amazonia, Brazil: Evidences in an SRTM digital elevation model. Remote Sensing of Environment, 110: 387-392.

Barros, S.V.A. 2010. Otimização dos usos múltiplos em pequenos açudes na bacia do açude de Sumé - PB. Programa de Pós-Graduação em Engenharia Civil e Ambiental, Universidade Federal de Campina Grande. Dissertação de Mestrado, 163 p.

Braga, A.C.O. 2016. Métodos elétricos em hidrogeologia. Editora Oficina de Textos. São Paulo, 159 p.

Cadier, E. 1994. Hidrologia das pequenas bacias do Nordeste semiárido: transposição hidrológica. SUDENE, Recife. 373p.

CPRM, 2000. Programa Levantamentos Geológicos Básicos do Brasil. Sumé. Folha SB.24-Z-D-V. Estados da Paraíba e Pernambuco. Escala 1:100.000.

DNOCS. 2018. Perímetro Irrigado de Sumé. Disponível em: www.dnocs.gov.br/~dnocs/doc/canais/perimetros_irrigados/pb/sume.htm. Acesso em: 05 de abril de 2018.

EMBRAPA. 2006. Centro Nacional de Pesquisa de Solos. Sistema Brasileiro de Classificação de Solos. 2 ed. Rio de Janeiro, 306 p.

Genau, R.B.; Madsen, J.A.; Mcgeary, S. & Wehmiller, J.F. 1994. Seismic-reflection identification of Susquehanna River paleochannels on the mid-Atlantic coastal plain. Quaternary Research, 42: 166-175.

Gilvear, D. & Bryant, R.G. 2003. Analysis of aerial photography and other remotely sensed data. In: KONDOLF, G.M.; PIEGAY, H. (ed.) Tools in Fluvial Geomorphology. Chichester: Wiley, p. 135-170.

Falgàs, E.; Ledo, J.; Benjumea, B.; Queralt, P.; Marcuello, A.; Teixidó, T. & Martí, A. 2011. Integrating hydrogeological and geophysical methods for the characterization of a deltaic aquifer system. Surv. Geophys., 32: 857–873.

Fradelizio, G.L.; Levander, A. & Zelt, C.A. 2008. Three-dimensional seismic-reflection imaging of a shallow buried paleochannel. Geophysics, 73: B85-B98.

Júnior, V.A.L.; Porto, R.Q.; Silans, A.M.B.P.; Almeida, C.N; Silva, G.S. & Santos, F.A. 2009. Estimativa do volume anual escoado de pequenos açudes no semiárido nordestino: um estudo de caso na bacia hidrográfica do açude de Sumé-PB. In: Simpósio Brasileiro de Recursos Hídricos, 18, Campo Grande.

Islam, Z.U.; Iqbal, J.; Khan, J.A. & Qazi, W.A. 2016. Paleochannel delineation using Landsat 8 OLI and Envisat ASAR image fusion techniques in Cholistan desert, Pakistan. J. Appl. Remote Sensing, 10: 046001-1 - 046001-17, DOI: 10.1117/1. JRS.10.046001.

Kafri, U. & Goldman, M. 2005. The use of the time domain electromagnetic method to delineate saline groundwater in granular and carbonate aquifers and to evaluate their porosity. J. Appl. Geophysics, 57(3): 167–178.

Krivochieva, S. & Chouteau, M. 2003. Integrating TDEM and MT methods for characterization and delineation of the Santa Catarina aquifer (Chalco Sub-Basin, Mexico). J. Appl. Geophysics, 52(1): 23–43.

Luciano, K.E. & Harris, M.S. 2013.Surficial geology and geophysical investigations of the Capers Inlet, South Carolina (USA) 7.5-Minute Quadrangle. Journal of Maps, 9: 115-120, DOI: 10.1080/17445647.2012.756831.

Meju, M.A.; Gallardo, L. & Mohamed, A.K. 2003. Evidence for correlation of electrical resistivity and seismic velocity in heterogeneous near-surface materials. Geophys. Res. Lett. 30(7): 26-1 – 26-4. DOI: 10.1029/2002 GL016048.

Montenegro, S.M.G.L.; Montenegro, A.A.A.; Mackay, R. & Oliveira, A.S.C. 2003. Dinâmica hidrosalina em aquífero aluvial utilizado para agricultura irrigada familiar em região semiárida. Revista Brasileira de Recursos Hídricos, 8: 85-92.

Mota, R. & Monteiro dos Santos, F. 2006. 2D sections of porosity and water saturation percent from combined resistivity and seismic surveys for hydrogeologic studies. The Leading Edge, 25: 735–737.

Pedersen, L.B.; Bastani, M. & Dynesius, L. 2005. Groundwater exploration using combined controlled-source and radiomagnetotelluric techniques. Geophysics, 70: G8–G15. DOI:10.1190/1.1852774.

Rossetti, D.F. 2010. Multiple remote sensing techniques as a tool for reconstructing late Quaternary drainage in the Amazon lowland. Earth Surf. Process. Landforms, 35: 1234–1239.

Salgado, J.P. 2016. Influência do lançamento de esgotos na qualidade das águas do aquífero aluvial do Rio Sucurú, no município de Sumé – PB. Programa de Pós-Graduação em Engenharia Civil e Ambiental, Universidade Federal de Campina Grande, Dissertação de Mestrado, 102p.

Schwinn, W. & Tezkan, B. 1997. 1D joint inversion of radiomagnetotelluric (RMT) and transient electromagnetic (TEM) data - an application for groundwater prospection in Denmark. In: EEGS, 3, Arhus.

Silva, L.F.D. 2006. Avaliação de unidades produtivas da agricultura familiar no perímetro irrigado de Sumé-PB. Programa de Pós- graduação em Engenharia Agrícola, Universidade Federal de Campina Grande, Dissertação de Mestrado, 89p.

Unsworth, M.J.; Lu, X. & Watts, M.D. 2000. AMT exploration at Sellafield: characterization of a potential radioactive waste disposal site. Geophysics, 65: 1070–1079.

Vieira, L.J.S. 2002. Emprego de um modelo matemático de simulação do fluxo subterrâneo para definição de alternativas de exportação de um aquífero aluvial. Programa de Pós-Graduação em Engenharia Civil e Ambiental, Universidade Federal de Campina Grande, Dissertação de Mestrado, 94 p.